# The inner nuclear membrane protein Src1 associates with subtelomeric genes and alters their regulated gene expression

Stefanie E. Grund,[1] Tamás Fischer,[1] Ghislain G. Cabal,[2] Oreto Antúnez,[3,4] José E. Pérez-Ortín,[3,4] and Ed Hurt[1]

[1]Biochemie-Zentrum der Universität Heidelberg, D-69120 Heidelberg, Germany
[2]Unité de Biologie Cellulaire du Noyau, Institut Pasteur, 75724 Paris, Cedex 15, France
[3]Departamento de Bioquímica y Biología Molecular and [4]Sección de Chips de DNA Servei de Suport a la Investigació Experimental, Universitat de València, E46100 València, Spain

Inner nuclear membrane proteins containing a LEM (LAP2, emerin, and MAN1) domain participate in different processes, including chromatin organization, gene expression, and nuclear envelope biogenesis. In this study, we identify a robust genetic interaction between transcription export (TREX) factors and yeast Src1, an integral inner nuclear membrane protein that is homologous to vertebrate LEM2. DNA macroarray analysis revealed that the expression of the phosphate-regulated genes *PHO11*, *PHO12*, and *PHO84* is up-regulated in *src1Δ* cells. Notably, these *PHO* genes are located in subtelomeric regions of chromatin and exhibit a perinuclear location in vivo. Src1 spans the nuclear membrane twice and exposes its N and C domains with putative DNA-binding motifs to the nucleoplasm. Genome-wide chromatin immunoprecipitation–on-chip analyses indicated that Src1 is highly enriched at telomeres and subtelomeric regions of the yeast chromosomes. Our data show that the inner nuclear membrane protein Src1 functions at the interface between subtelomeric gene expression and TREX-dependent messenger RNA export through the nuclear pore complexes.

## Introduction

Among the numerous steps of gene expression, formation, and maturation of messenger RNP particles (mRNPs) are crucial steps before transcripts can be exported from the nucleus and translated in the cytoplasm. Studies over the past years have revealed that these various steps, including gene activation, transcription, 5′ capping, 3′ end processing and polyadenylation, splicing, mRNA surveillance/quality control, and export of mRNPs are tightly coupled (for reviews see Reed and Cheng, 2005; Sommer and Nehrbass, 2005).

In the yeast *Saccharomyces cerevisiae*, the THO–transcription export (TREX) complex and the Sac3–Thp1–Sus1–Cdc31 (TREX-2) complex are involved in transcription-coupled mRNA export (for reviews see Reed and Cheng, 2005; Köhler and Hurt, 2007). The THO–TREX complex is thought to be recruited to the elongating RNA polymerase II complex via the THO subunits (Hpr1, Tho2, Mft1, and Thp2), which preferentially function in transcription and packaging of nascent mRNA, whereas the other TREX factors Sub2 and Yra1 are involved in recruiting the Mex67-Mtr2 export receptor to the mRNP, thereby coupling mRNP biogenesis with mRNA export (for reviews see Reed and Cheng, 2005; Köhler and Hurt, 2007). The TREX-2 complex potentially coordinates Spt/Ada/Gcn5 acetyltransferase (SAGA)–mediated transcription of certain genes at the inner nuclear side of the nuclear pore complex (NPC; Rodríguez-Navarro et al., 2004). A key factor of TREX-2 is the Sac3 subunit, a multidomain protein that binds the remaining complex members. Sac3 associates with Thp1, which was initially found to be involved in transcription elongation (Gallardo and Aguilera, 2001), and with Sus1 and Cdc31 via its CID (Cdc31-interacting domain) motif (Fischer et al., 2004). Moreover, Sac3 can also directly bind to the export receptor Mex67-Mtr2 (Fischer et al.,

Correspondence to Ed Hurt: ed.hurt@bzh.uni-heidelberg.de

Abbreviations used in this paper: 5-FOA, 5-fluoroorotic acid; ChIP, chromatin immunoprecipitation; HP, high phosphate; LP, low phosphate; mRNP, messenger RNP particle; MSC, Man1-Src1 C terminal; NPC, nuclear pore complex; ProtA, protein A; rDNA, ribosomal DNA; SAGA, Spt/Ada/Gcn5 acetyltransferase; TAP, tandem affinity purification; TEV, tobacco etch virus; TREX, transcription export; wt, wild type.

The online version of this article contains supplemental material.



The Rockefeller University Press $30.00
J. Cell Biol. Vol. 182 No. 5 897–910
www.jcb.org/cgi/doi/10.1083/jcb.200803098

2002; Lei et al., 2003). In vivo, the TREX-2 complex is predominantly located at the NPC, which requires the nuclear basket nucleoporin Nup1 (Fischer et al., 2002). Notably, the TREX-2 factor Sus1 is also a component of the chromatin-bound SAGA complex involved in transcription initiation of a subset of genes (Rodríguez-Navarro et al., 2004) and part of a SAGA module, which is involved in deubiquitination of H2B (Köhler et al., 2006). Thus, Sus1 could be a bridging factor between the SAGA transcription machinery and the NPC-associated TREX-2 complex.

Historically, the nuclear periphery was known as a zone that harbors silenced regions of the genome and thus was believed to be an area of transcription repression. However, recent studies have revealed that genes can be recruited to the nuclear periphery upon their transcriptional activation (for reviews see Akhtar and Gasser, 2007; Köhler and Hurt, 2007). Thus, activating and repressing chromatin environments coexist but appear to be spatially partitioned. Whereas the heterochromatin, like telomeres and the mating-type locus, line the nuclear envelope, the active chromatin domains are in the vicinity of the NPCs (Taddei et al., 2004; for review see Akhtar and Gasser, 2007).

Gene recruitment to the nuclear periphery involves components of the nuclear basket and associated factors implicated in transcription and mRNA export, including SAGA and TREX-2 factors as well as Mex67. Regarding the mechanism, gene gating requires the nascent transcript or posttranscriptional events. However, other studies suggest that gene gating can also be independent of transcription and is then mediated by direct interaction of the gene with components of the nuclear periphery (for reviews see Akhtar and Gasser, 2007; Köhler and Hurt, 2007). In general, gene recruitment to the periphery could allow access to a favorable environment, including chromatin remodeling, transcription, and export machineries, thereby optimizing gene expression and mRNA export (for reviews see Akhtar and Gasser, 2007; Köhler and Hurt, 2007).

In this study, we found Src1 (also called Heh1; King et al., 2006) in genetic screens using mutants of the THO–TREX and TREX-2 complexes. Src1 exhibits a domain organization similar to higher eukaryotic LEM2 and MAN1, which are integral inner nuclear membrane proteins that consist of an N-terminal LEM domain, two transmembrane-spanning sequences, and a Man1-Src1 C-terminal (MSC) domain (Mans et al., 2004; Brachner et al., 2005). LEM proteins (named after LAP2, emerin, and MAN1) can interact with the nuclear lamina and/or chromatin-binding factors, thereby providing anchoring sites for chromatin at the nuclear periphery and modulating higher order chromatin structure (for reviews see Gruenbaum et al., 2005; Wagner and Krohne, 2007). Our analyses further revealed that Src1 is an integral membrane protein that spans the inner nuclear membrane twice, thereby exposing the putative DNA-binding N and C domains to the nucleoplasm. As shown by chromatin immunoprecipitation (ChIP)–on-chip analysis, Src1 is associated with subtelomeric regions that are located at the nuclear periphery. Moreover, the regulation of expression of genes located in the subtelomeric regions (e.g., *PHO11*, *PHO12*, and *PHO84*) is altered in cells lacking Src1. These data suggest that Src1 functions at the interface between chromatin organization of subtelomeric genes at the inner nuclear membrane and TREX-dependent mRNA export.

## Results

### TREX factors interact genetically with *SRC1*

To unravel the genetic network in which TREX factors carry out their function in vivo, we performed synthetic lethal screens with the mutant strains *hpr1*Δ (a THO–TREX factor), which is thermosensitive for growth at 37°C, and *thp1*Δ (a TREX-2 factor). Each screen yielded a synthetic lethal mutant that was complemented by *SRC1* (unpublished data). DNA sequencing of the *SRC1* allele recovered from the *thp1*Δ synthetic lethal mutant indeed revealed that Src1 was inactivated in the synthetic lethal strain by a premature stop codon at amino acid 455 (unpublished data). *SRC1* was previously identified as an intron-containing gene involved in sister chromatid segregation (Rodríguez-Navarro et al., 2002). In another study, Src1/Heh1 was shown to be located at the inner side of the nuclear membrane (King et al., 2006). To directly verify the identified genetic interactions, we combined the nonessential *src1*Δ (null) allele with the nonessential *thp1*Δ or *hpr1*Δ disruption alleles. This analysis confirmed that the generated double mutants, *src1*Δ*thp1*Δ and *src1*Δ*hpr1*Δ, were not viable (i.e., synthetic lethal; Fig. 1).

To gain further insight in the genetic network in which *SRC1* is active, we tested additional factors with known roles in transcription-coupled mRNA export for a functional overlap with *SRC1*. This analysis indicated that *SRC1* is genetically linked to another TREX-2 factor *SAC3* (Fig. 1) but not to *SUS1* or *CDC31* (Fig. 1 and not depicted). This correlates with the fact that *src1*Δ is not synthetic lethal with *sac3*ΔCID, where the binding site for Sus1 and Cdc31 is deleted (Fig. 1). Unexpectedly, the other THO–TREX mutants *tho2*Δ, *mft1*Δ, and *thp2*Δ were not found to be genetically linked to *src1*Δ (Fig. 1 and not depicted). Moreover, factors acting more downstream in transcription-coupled mRNA export (e.g., mutants of *YRA1* or *MEX67)* and *mlp1*Δ*mlp2*Δ were not synthetic lethal with *src1*Δ (unpublished data). In contrast, a synthetically enhanced growth inhibition was observed between *src1*Δ and the *sub2-85* allele (Fig. 1). Collectively, these genetic studies indicated that *SRC1* is functionally linked to factors of the THO–TREX and TREX-2 complex, and thus, Src1 might functionally overlap with an upstream step in the formation of an export-competent mRNP.

### Two forms of Src1 protein generated by alternative splicing are functionally not equivalent

To study the in vivo role of Src1 with respect to its genetic linkage to TREX factors, we sought to tag chromosomal *SRC1* at the C terminus with the tandem affinity purification (TAP) and GFP tag to perform affinity purification and subcellular location experiments, respectively. However, C-terminal tagging was not straight forward because *SRC1* contains an intron that can be alternatively spliced (Davis et al., 2000; Rodríguez-Navarro et al., 2002).

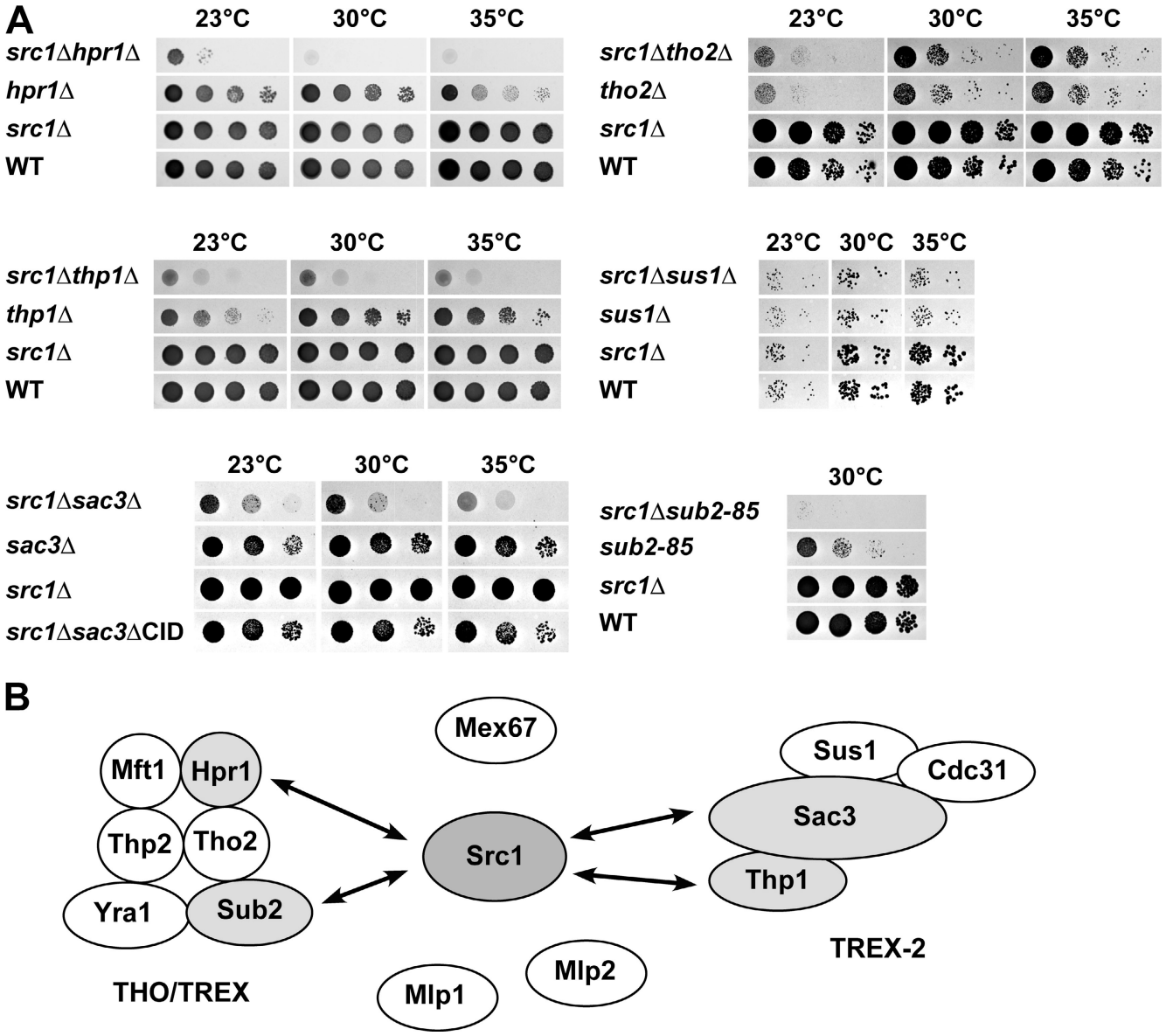


Figure 1. **Genetic interaction of *SRC1* with THO–TREX and TREX-2 members.** (A) The double-disrupted strains were transformed with the respective plasmid-borne wt or mutant genes. Growth was analyzed by spotting transformants in 10-fold serial dilutions on 5-FOA–containing plates at the indicated temperature for 5 d or on synthetic dextrose complete–Leu-Trp for 3 d (*src1Δsub-85*, *src1Δtho2Δ*, and *src1Δsus1Δ*). No growth indicates synthetic lethality. (B) Schematic representation of the genetic network between *SRC1* and factors involved in transcription-coupled mRNA export. Arrows to gray components indicate synthetic lethality/enhancement, and proteins depicted in white are genetically not linked to *SRC1*.

Specifically, the *SRC1* intron has two alternative 5′ splice sites, which could potentially encode two different Src1 proteins: a long form with 834 (Src1-L) and a shorter form with 687 amino acids (Src1-S). Importantly, Src1-L and Src1-S would differ in their amino acid sequences at the C-terminal end because the alternative 5′ splice sites shift the reading frame in the 3′ exon (Fig. 2 A).

To demonstrate that both Src1 splice variants are produced in vivo, we inserted the TAP tag at the two alternative stop codons by homologous recombination (Fig. 2 A). Both Src1-L and Src1-S were detected in about equimolar amounts in whole cell lysates (Fig. 2 B). Moreover, N-terminal TAP tagging of Src1 showed that both Src1 splice forms were coexpressed in similar ratios (Fig. 2 B). Notably, Src1-L and Src1-S do not have identical functions, as the long form of Src1 complements the synthetic lethal phenotype of THO–TREX and TREX-2 mutants significantly better than the short form (Fig. 2 C).

To find out whether both Src1s have a similar subcellular location, we performed fluorescence microscopy. Both Src1-L and Src1-S tagged at the N terminus with GFP exhibited a distinct concentration at the nuclear envelope with no apparent staining of other cellular membranes (Fig. S1, left, available at http://www.jcb.org/cgi/content/full/jcb.200803098/DC1). Moreover, Src1-L and Src1-S did not cluster with NPCs in the NPC-clustering *nup133*Δ mutant (Fig. S1, right). Thus, Src1-L and Src1-S are located at the inner nuclear membrane and appear not to have stable physical contact to the NPCs, although a transient interaction cannot be excluded.

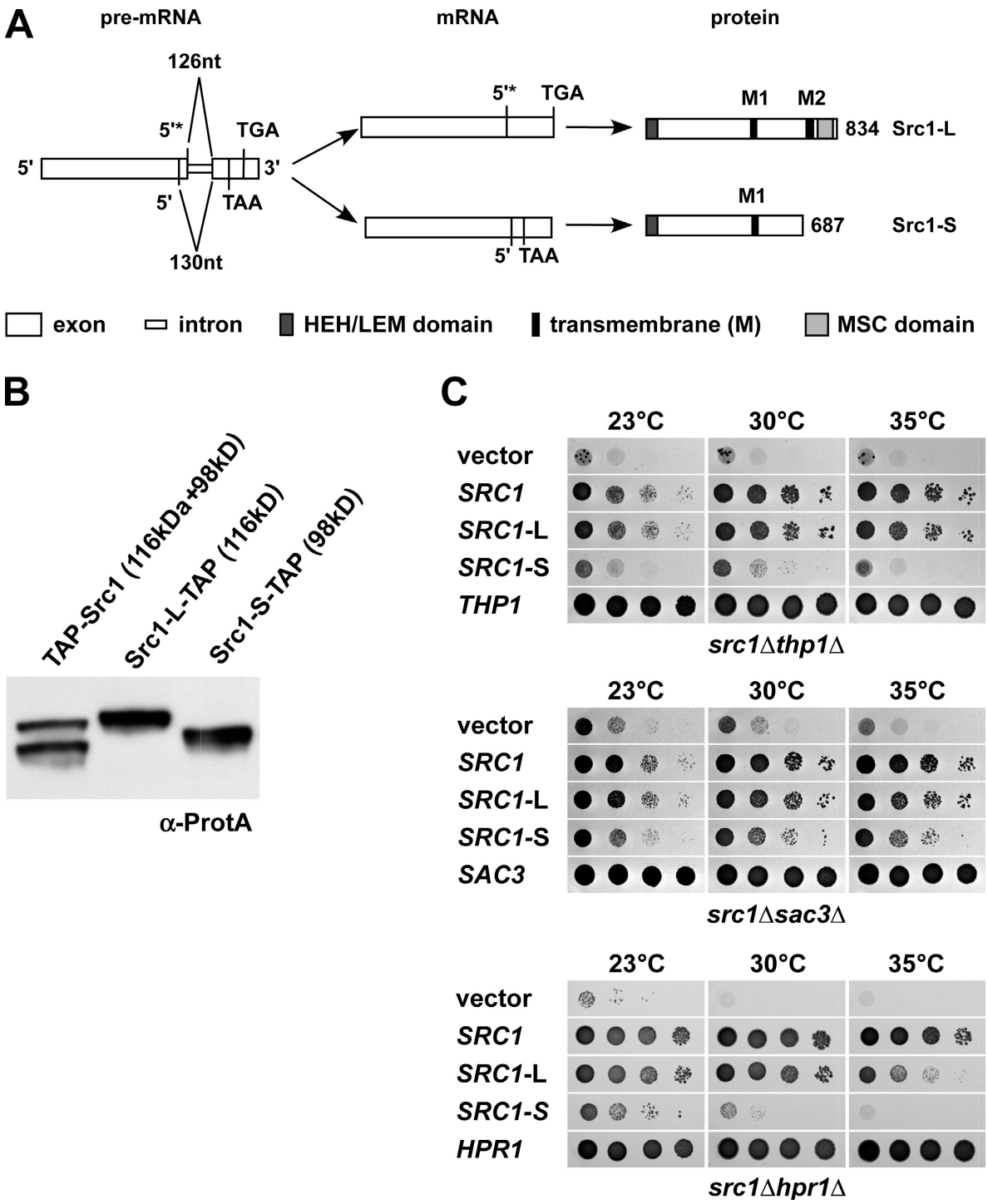


Figure 2. **Alternative splicing of *SRC1* results in two different spliced protein forms.** (A) Schematic overview of pre-mRNA, mRNA, and protein products upon alternative splicing. Either a 126- or a 130-nt intron can be excised by using two alternative 5′ splice sites. In the latter case, a frame shift results in an earlier stop codon and, therefore, in a shorter protein with a different amino acid sequence at the C terminus compared with Src1-L. Conserved domains (HEH/LEM and MSC) and transmembrane domains (M) are indicated. Numbers represent amino acid residues. (B) Whole cell lysates of N- (TAP-Src1) and C-terminal TAP-tagged Src1-L or Src1-S were analyzed by SDS-PAGE followed by Western blotting using anti-ProtA antibodies. (C) Genetic relationship of *SRC1* splice variants with TREX–THO and TREX-2 components. The double-disruption strains were transformed with empty vector, GFP-Src1 splice variants, and the respective TREX component. Transformants were spotted in 10-fold serial dilutions on 5-FOA–containing plates for 5 d at the indicated temperatures.

### Src1-L and Src1-S are integral inner nuclear membrane proteins with different topology

Biocomputational analysis suggested that Src1-L could be a membrane protein with two membrane-spanning sequences, but only the first transmembrane span has a strong prediction (Fig. 3 A). To experimentally verify that Src1-L is an integral membrane protein, whole cell lysates containing Src1-TAP were extracted under different conditions, and the partitioning of Src1-TAP into soluble and insoluble (membrane) fractions was tested and compared with

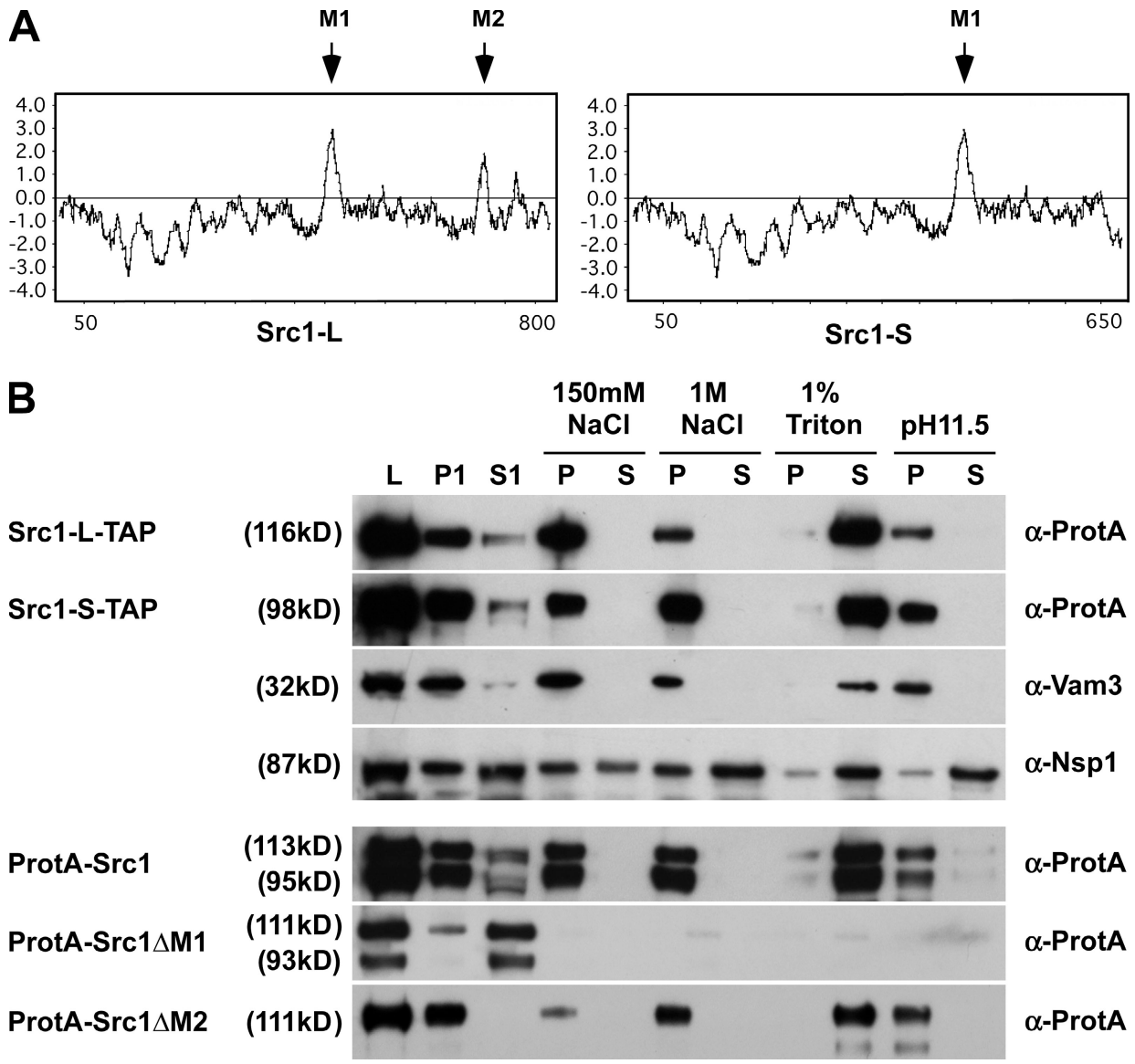


Figure 3. **Src1-L and Src1-S are integral membrane proteins.** (A) Kyte-Doolittle hydropathy analysis (with a 19–amino acid window size; Kyte and Doolittle, 1982) revealed two putative hydrophobic transmembrane-spanning regions (M1 and M2) for Src1-L but only one region with significant transmembrane potential for Src1-S. The hydrophobicity scores are plotted against the window number. (B) Crude membrane fractions from cells expressing Src1-L–TAP or Src1-S–TAP were extracted using four different conditions: 150 mM NaCl, 1 M NaCl, 1% Triton X-100, or pH 11.5. Equivalent amounts of fractions from lysate (L), membrane (P1), soluble (S1), and, after ultracentrifugation, insoluble pellet (P) and supernatant (S) were analyzed by SDS-PAGE followed by Western blotting with antibodies against ProtA, Vam3, and Nsp1. Western blotting against Vam3 and Nsp1 is only shown for Src1-S–TAP (top). Extraction profile of *src1*Δ cells harboring intron-containing constructs of ProtA-Src1 full length and deletion of the first (Src1ΔM1) or second (Src1ΔM2) hydrophobic stretch. Western blots were probed with an anti-ProtA antibody (bottom).

the behavior of a peripheral membrane protein (Nsp1) and an integral membrane protein (vacuolar Vam3). Whereas high salt (1 M NaCl) or pH 11.5 treatment did not release Src1-L and Src1-S, detergent (Triton X-100) efficiently solubilized both Src1-TAP splice variants, as with Vam3 (Fig. 3 B). Thus, the biochemical behavior of Src1 is typical of an integral membrane protein.

Because the putative transmembrane span M2 (residues 708–725) of Src1 has a lower hydrophobicity than transmembrane span M1 (residues 450–474) and M2 is absent from the Src1-S form because of alternative splicing (Fig. 3 A), we wanted to analyze the topology of both Src1 forms within the inner nuclear membrane in living cells (see models in Fig. 4 A). Thus, we developed a novel in vivo assay to probe for the topology of Src1-L and Src1-S within the inner nuclear membrane. Src1 was genomically TAP tagged at the N terminus (protein A [ProtA]–tobacco etch virus [TEV]–calmodulin-binding peptide–Src1) or C terminus (Src1–calmodulin-binding peptide–TEV-ProtA). The accessible TEV cleavage site in these constructs could be exploited to test whether it is cleaved by an inducible TEV protease carrying an NLS and a myc tag. We anticipated that the TEV protease should remove the ProtA moiety only from those Src1 constructs in which the epitope is exposed to the nucleoplasm but not when hidden in the perinuclear space (Fig. 4 B, left). When cells were grown in glucose (no TEV expression), all Src1 constructs retained the ProtA epitope, as shown by Western blotting with anti-ProtA antibodies (Fig. 4 B, lanes 1, 3, and 5).

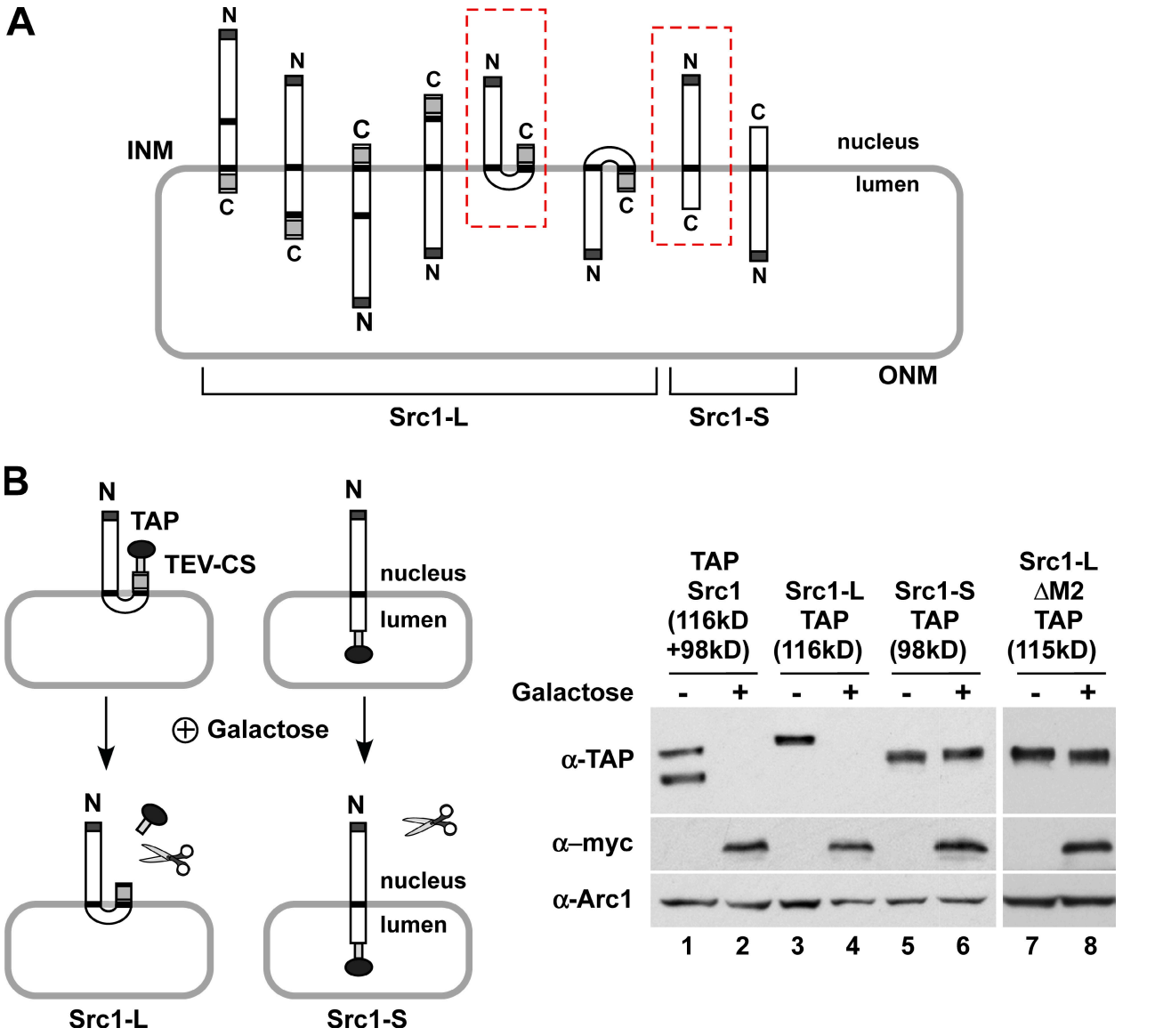


Figure 4. **Src1-L is a double-pass integral membrane protein, and Src1-S is a single-pass integral membrane protein.** (A) The six possible topological orientations for Src1-L and the two for Src1-S are shown. N, N terminus; C, C terminus; INM, inner nuclear membrane; ONM, outer nuclear membrane. Experimentally determined topologies are boxed in red. (B) Schematic illustration of the TEV-based method to determine the topology of Src1 membrane insertion (left). Under inducing conditions, the TEV protease is expressed and cleaves at TEV cleavage sites when accessible at the nuclear side. TEV-CS, TEV cleavage site. Cells expressing N- (TAP-Src1) or C-terminal TAP-tagged Src1 (Src1-L–TAP and Src1-S–TAP) or *src1*Δ cells containing C-terminal TAP-tagged Src1-L–ΔM2 were grown either under noninducing (−) or inducing (+) conditions (right). Whole cell extracts were analyzed by Western blotting using anti-ProtA, anti-myc (TEV protease), and anti-Arc1 antibodies (loading control).

When cells were shifted to galactose to induce the TEV protease, both short and long N-terminally tagged Src1 as well as C-terminally tagged Src1-L lost their ProtA tags, suggesting that the N terminus of Src1-L and Src1-S and the C terminus of Src1-L are facing the nucleoplasm (Fig. 4 B, lanes 2 and 4). However, the TEV protease could not remove the ProtA epitope from the C-terminally tagged Src1-S (Fig. 4 B, lane 6). Altogether, these data suggest that Src1-L spans the inner nuclear membrane twice with the N and C domain exposed to the nucleoplasm (Fig. 4 A, boxed in red). In contrast, Src1-S spans the membrane once with the N domain located in the nucleoplasm and a short C-terminal domain hidden in the perinuclear space (Fig. 4 A, boxed in red).

### Role of the various Src1 domains for membrane insertion and nuclear envelope targeting

To determine the contribution of the transmembrane spans M1 and M2 for membrane insertion of Src1, mutants lacking M1 or M2 were expressed in the *src1*Δ mutant and subsequently analyzed in vitro and in vivo. Biochemical studies revealed that Src1ΔM2 behaved like an integral membrane protein, whereas Src1ΔM1 was no longer inserted into the membrane and became soluble (Fig. 3 B). Thus, M1 is necessary and sufficient for membrane insertion of Src1. However, M2 alone could not confer a stable membrane insertion and only integrated into the nuclear membrane in the context of full-length Src1 (Fig. 4 B).

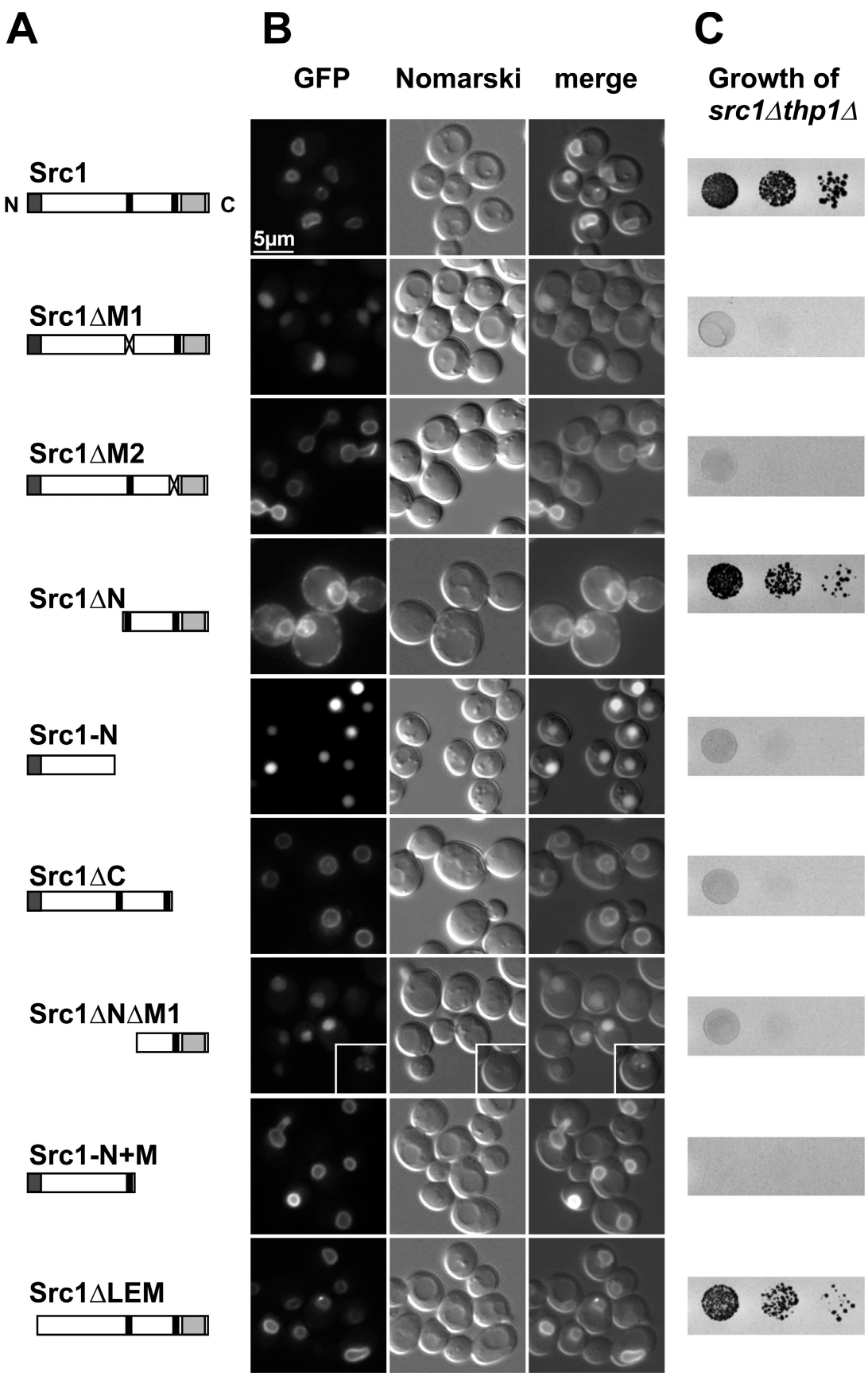


Figure 5. **Src1 domain analysis.** (A) Schematic representation of Src1 deletion constructs. (B) Fluorescence microscopy of *src1*Δ cells harboring the indicated GFP-tagged Src1 full-length and truncation constructs. (C) The double-disruption strain *src1*Δ*thp1*Δ carrying plasmid-borne *THP1* was transformed with the indicated constructs, and cells were spotted in 10-fold serial dilutions on 5-FOA–containing plates and incubated for 5 d at 30°C. Only cDNA-based constructs of Src1-L are shown.

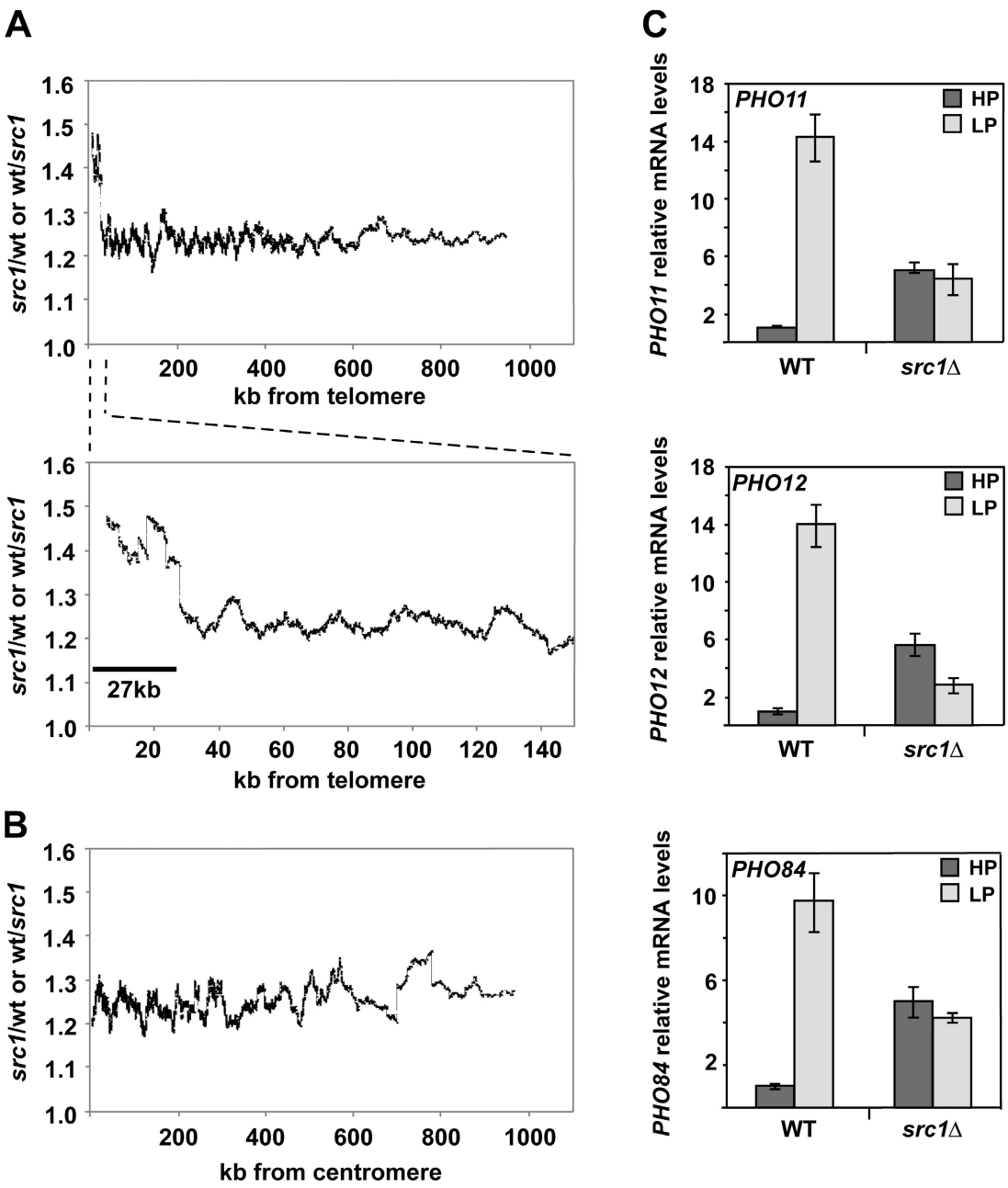


Figure 6. **Analysis of gene expression in the *src1*Δ mutant.** (A and B) Relative increases (*src1*/wt, when *src1* > wt) or decreases (wt/*src1*, when *src1* < wt) of gene expression were plotted versus their distance to the closest telomere (A) or centromere (B). A sliding window of 100 genes was used. The average of the 100 genes was used for the y axis, and the distance of the central gene in the window was used for the x axis. The bottom panel of A is an expanded view of the top graph showing the ~27-kb region close to the telomeres, which exhibits a misregulation in the *src1* deletion strain. (C) Expression levels of *PHO* mRNAs in wt and *src1*Δ cells. Total RNA of wt and *src1*Δ cells grown in HP and LP was prepared, and cDNA was analyzed by quantitative RT-PCR using specific primers for *PHO11*, *PHO12*, and *PHO84*. Each gene was assayed in triplicates. The mRNA levels of wt HP expression are set as one. One representative dataset of five times independently isolated RNA is shown. Error bars represent SD.

Thus, the first transmembrane domain in Src1 is necessary for membrane insertion, whereas the second membrane span alone cannot confer integral insertion into the membrane but develops insertion activity when M1 is present.

To study the role of the transmembrane sequences M1 and M2 and of other domains for nuclear envelope targeting of Src1 in vivo, GFP-tagged Src1 mutant constructs (Fig. 5 A) were analyzed for their subcellular location by fluorescence microscopy (Fig. 5 B). This analysis showed that GFP-Src1ΔM2 was still located at the nuclear envelope, in contrast to GFP-Src1ΔM1, which was detached from the nuclear periphery and mislocalized to the nucleoplasm.

Consistent with these findings, the N-terminal domain of Src1 devoid of any membrane span showed a strong nuclear accumulation. The reciprocal construct, GFP-Src1ΔN, was still targeted to the nuclear envelope, albeit with lower efficiency, and was partly found to be associated with other membranes (cortical ER or plasma membrane). Deletion of only the N-terminal

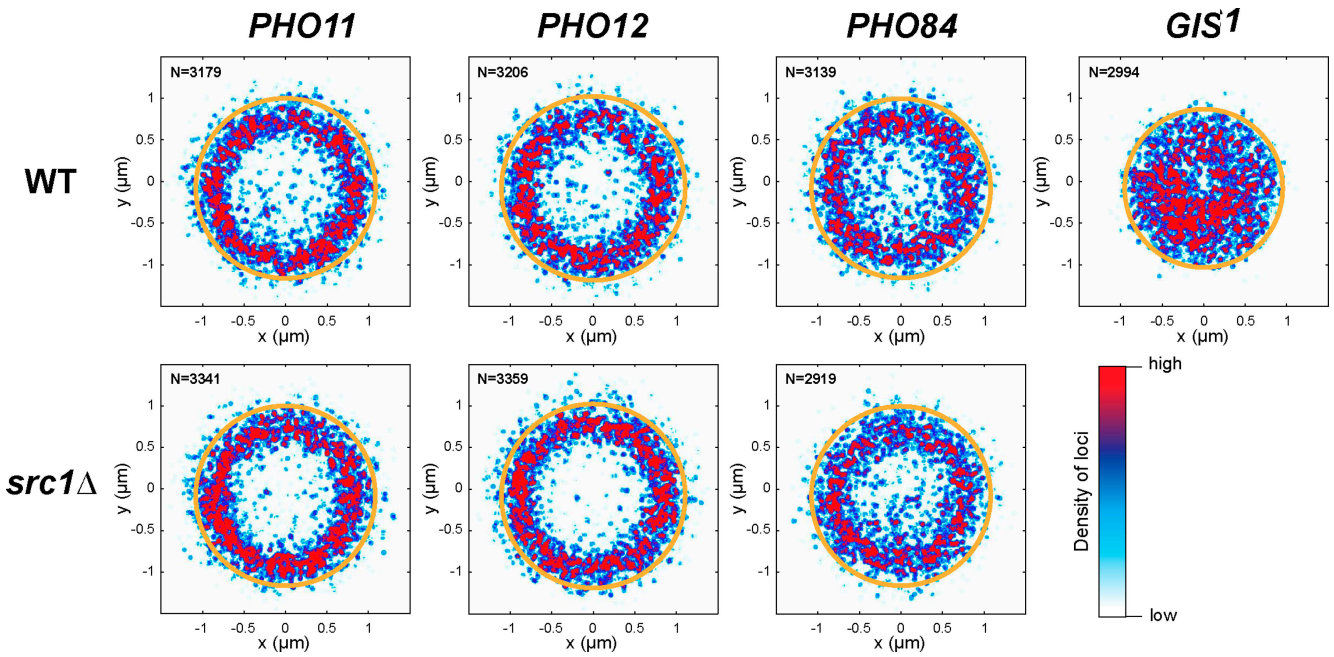


Figure 7. **In vivo localization of *PHO* gene loci.** 3D localization of TetO/TetR-GFP–labeled *PHO11*, *PHO12*, *PHO84*, and *GIS1* loci in wt or *src1*Δ cells expressing GFP-Nup49 was determined after microscopy acquisition in vivo (see Materials and methods). For each strain, positions of the loci obtained from N nuclei are plotted in radial projection on the same graph (as previously described in Cabal et al., 2006). Hot colors indicate high density of loci, and cold colors indicate low density (the color scale is indicated on the bottom right). Average outlines of the nuclear envelope (orange circles) are also shown.

LEM domain (ΔLEM) did not affect the nuclear envelope location of Src1. Notably, the Src1ΔNΔM1 construct was also located in the nucleoplasm with occasional perinuclear spots. Altogether, the data suggest that the N domain and, to a lesser extent, also the C domain of Src1-L contribute to nuclear targeting, whereas the first transmembrane domain is necessary and sufficient to insert Src1 into the inner nuclear envelope.

To assess which Src1domains are functionally important, we tested the ability of the different truncated Src1 forms to complement the synthetic lethal phenotype of the *src1*Δ*thp1*Δ double mutant (Fig. 5 C). None of the constructs, which lacked either M1 or M2, complemented the *src1*Δ*thp1*Δ strain. Thus, although Src1ΔM2 apparently is targeted to and inserted into the nuclear membrane, it is not functional in our complementation assay. Notably, the C-terminal domain of Src1-L is exposed to the nucleoplasm (see previous section), but in the Src1ΔM2 strain it is hidden in the lumen of the perinuclear space (Fig. 4 B). Thus, the C-terminal domain of Src1 performs a crucial role with respect to the Thp1 function and has to be both targeted to the membrane and exposed to the nucleoplasm. In contrast, Src1 devoid of the LEM domain or the entire N terminus is able to significantly complement the *src1*Δ*thp1*Δ strain and thus may perform additional functions.

### Src1 is involved in expression of subtelomeric *PHO* genes that exhibit a perinuclear location

As Src1 was found in this study to be linked to TREX factors, we determined whether Src1 participates in transcription and/or mRNA export. In situ hybridization using fluorescently labeled oligo(dT) nucleotide probes did not reveal a nuclear mRNA export defect in *src1*Δ cells (unpublished data), consistent with the finding that Src1 is not genetically linked to mRNA export factors such as Mex67 (see the first Results section). To investigate whether Src1 plays a role in transcription, we analyzed the expression profile of the ∼6,000 yeast genes in the *src1Δ* strain using DNA macroarrays. This genome-wide analysis indicated that only a small number of genes (∼60) is affected in the *src1*Δ mutant (increased or decreased expression), which also included genes that have a subtelomeric location (Table S1, available at http://www.jcb.org/cgi/content/full/jcb.200803098/DC1; and Gene Expression Omnibus database). To analyze whether subtelomeric genes have a higher probability to be affected in their expression than other genes when *SRC1* is deleted, the relative increases (*src1*/wild type [wt] when *src1* > wt) or decreases (wt/*src1* when *src1* < wt) of gene expression were plotted versus their distance to the closest telomere or centromere using a sliding window of 100 genes. This analysis suggested a statistically significant misregulation of subtelomeric genes in *src1*Δ cells (subtelomeric regions are defined to be within ∼25 kb from each telomere; Fig. 6 A; Louis, 1995). This effect is specific to telomeres because it does not occur (e.g., in regions close to the centromeres; Fig. 6 B). In particular, several *PHO* genes (*PHO84*, *PHO11*, *PHO12*, and, to a lesser extent, also *PHO4*) were markedly up-regulated in cells devoid of Src1 (Table S1). Quantitative real-time PCR independently showed that *PHO84, PHO11*, and *PHO12* transcript levels increased approximately fivefold in *src1*Δ cells when grown in high phosphate (HP) medium. However, further up-regulation of these *PHO* genes was no longer observed in *src1*Δ cells when shifted from high to low

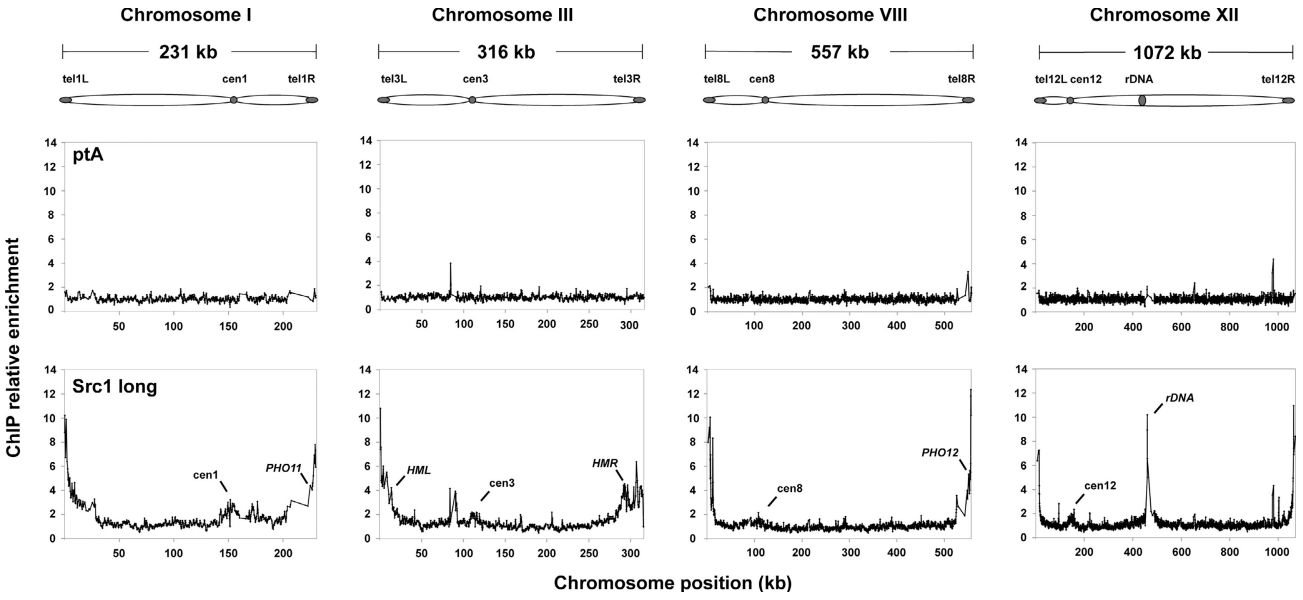


Figure 8. **Genome-wide distribution maps of Src1.** ChIP-on-chip analyses were performed to identify the global targets of Src1-L across the *S. cerevisiae* genome. Relative enrichments of ProtA-Src1 or ProtA as a control are plotted in alignment with the map of each chromosome. For simplicity, only four representative chromosomes are shown. Localization of *PHO11* and *PHO12*, the rDNA locus, and the two mating-type loci is shown. cen, centromere; HML/HMR, mating-type loci; tel, telomere.

phosphate (LP) medium (Fig. 6 C). In contrast, *PHO84*, *PHO11*, and *PHO12* transcript levels were low in wt cells when grown in HP medium but could be significantly up-regulated upon transfer to LP medium (Fig. 6; for review see Oshima, 1997). Altogether, these analyses indicated that deletion of *SRC1* leads to a disturbed regulation of gene expression of a group of *PHO* genes, which encode a phosphate transporter in the plasma membrane and secreted acid phosphatases.

Notably, the *PHO84*, *PHO11*, and *PHO12* genes that exhibit altered gene expression in the *src1*Δ strain are all located in subtelomeric regions of the chromosomes (Table S1). It is well known that telomeres are preferentially located at the nuclear periphery in yeast (Klein et al., 1992); thus, we wanted to localize the subtelomeric *PHO84*, *PHO11*, and *PHO12* gene loci with regard to the nuclear envelope in live cells. As a control, a randomly selected region that was not proximal to telomeres but was close to the interchromosomal *GIS1* locus was investigated. Thus, TetO repeats were inserted close to the *PHO11*, *PHO12*, *PHO84*, or *GIS1* chromosome loci, and TetR-GFP was expressed to visualize the TetO-labeled genes. This analysis showed that all of the three gene loci, *PHO11*, *PHO12*, or *PHO84,* are positioned at the nuclear periphery, whereas *GIS1* is distributed predominantly in the nucleoplasm (Fig. 7). However, the observed nuclear envelope tethering of the *PHO* genes did not require Src1, as the perinuclear location of these gene loci was not altered in *src1*Δ cells (Fig. 7). Collectively, the data showed that Src1 is involved in gene expression of a class of *PHO* genes that are located in subtelomeric regions and in vivo exhibit a perinuclear location.

## Src1 is associated with subtelomeric chromatin

To identify molecules, which potentially link Src1 to chromatin, we sought to affinity purify ProtA-Src1. Although ProtA–Src1-L or –Src1-S could be significantly enriched using a protocol for isolation of membrane proteins, coenrichment of stoichiometrically interacting proteins was not observed (Fig. S2, available at http://www.jcb.org/cgi/content/full/jcb.200803098/DC1).

Next, we tested whether ProtA-Src1 is associated with chromatin. We performed genome-wide ChIP-on-chip analyses to determine the chromosomal distribution profile of Src1-L. Overall, three independent ChIP-on-chip experiments were performed with ProtA-Src1, and the data were highly similar. As shown in Fig. 8 and Fig. S3 (available at http://www.jcb.org/cgi/content/full/jcb.200803098/DC1) for one set of these experiments, a significant enrichment of Src1 at subtelomeric regions of all 16 yeast chromosomes was observed (note that the genomic chips used in this study did not contain the repetitive telomeric DNA). Moreover, Src1 localizes also to other heterochromatin-like regions such as the ribosomal DNA (rDNA) locus, the mating-type loci (within subtelomeric regions of chromosome III), and, albeit only to a minor degree, to centromeric regions (Fig. 8). Most of the other locations to which Src1 maps to a minor extent are likely to be unspecific, as those loci are also enriched in the ProtA control. Altogether, these data indicate that Src1 is preferentially associated with subtelomeric chromatin, and this interaction can affect expression of subtelomeric-located genes.

To test whether Src1 plays a role in gene silencing, we monitored the expression of a silenced *URA3* reporter inserted into the telomeric region of chromosome 7 in the presence and absence of *SRC1*. Deletion of *SRC1* did not affect telomeric silencing as revealed by a normal growth of cells on 5-fluoroorotic acid (5-FOA)–containing plates in comparison with a wt strain. In contrast, when *yku70*Δ cells known to have a telomeric silencing defect (Laroche et al., 1998) were plated on 5-FOA, a significant growth inhibition was observed. Moreover, the combination of *src1*Δ and *yku70*Δ in haploid cells caused a

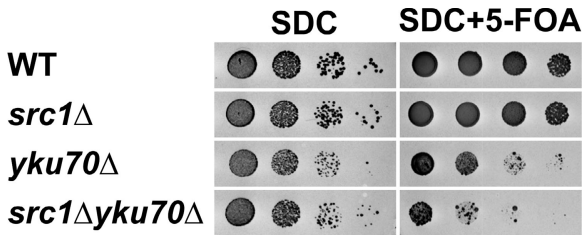


Figure 9. ***src1*Δ cells are not affected in telomere silencing, but in combination with the *yku70*Δ mutation, they are synergistically impaired.** Deletions of *SRC1*, *YKU70*, or double deletion in a telVIIL::*URA3* strain were spotted in 10-fold serial dilutions on 5-FOA–containing plates and grown for 5 d at 23°C. Note that growth reflects telomeric silencing and reduced growth derepression of silencing. Synthetic dextrose complete without 5-FOA was used as a plating control.

synergistic inhibition of growth on 5-FOA plates (Fig. 9). These data suggest that Src1 in combination with another silencing factor can synergistically affect telomeric silencing.

## Discussion

This study has revealed that the integral inner nuclear membrane protein Src1 functions in gene regulation of subtelomeric genes and is embedded functionally in a network of factors, which participate in transcription-coupled mRNA export. Importantly, Src1 is associated with subtelomeric chromatin and thus can help to organize this region of the chromosomes. In previous studies, Src1 was shown to contain an intron with the possibility of alternative splicing (Davis et al., 2000; Rodríguez-Navarro et al., 2002). Our study revealed that both splice forms localize to the nuclear periphery and are integral inner nuclear membrane proteins (King et al., 2006). However, both proteins are not functionally equivalent. To the best of our knowledge, this is the first demonstration that two forms of a protein generated by alternative splicing in yeast have different functions.

The N domain of Src1 mediates nuclear targeting, and insertion into the nuclear membrane requires the first transmembrane span. These findings are consistent with studies of vertebrate LEM2 and MAN1 in which nuclear envelope targeting and retention are also dependent on the first transmembrane domain and the N terminus (Wu et al., 2002; Brachner et al., 2005). Previously, it has been shown that Src1 is imported to the inner nuclear membrane by the Kap60–Kap95 pathway in a RanGTP-dependent manner (King et al., 2006). Replacing the entire N terminus of Src1 with the classical SV40 NLS, however, was not sufficient to restore its normal localization at the inner nuclear membrane (unpublished data). This suggests that besides an NLS, additional targeting/retention information is retained within the N domain of Src1.

Src1 is preferentially associated with heterochromatin such as subtelomeric and telomeric chromatin. As both N- and C-terminal domains of Src1-L face the nucleoplasm and each harbors a potential DNA-interacting domain (LEM and MSC), it is possible that the interaction with DNA is direct, but adaptor proteins could also be involved in chromatin binding. LEM domain proteins in higher eukaryotes are able to associate with chromatin either directly (Cai et al., 2001; Caputo et al., 2006) or via the chromatin-associated barrier to autointegration factor (for review see Wagner and Krohne, 2007). However, a homologue of barrier to autointegration factor does not exist in yeast, and we were unable to find stoichiometric protein interaction partners of Src1.

Telomeres are anchored to the nuclear periphery in yeast by redundant mechanisms involving the heterodimeric yKu complex and Sir4, which associates with the membrane-associated Esc1 (Hediger et al., 2002; Taddei et al., 2004). Moreover, the SUN domain protein Mps3 assists in Sir4-dependent telomere tethering and silencing (Bupp et al., 2007). Whether Src1 functions directly in silencing remains open. *SRC1* is not genetically linked to *ESC1* or *YKU70* (unpublished data), and telomere silencing was not affected in *src1*Δ cells. However, disruption of *SRC1* affected telomere length (Askree et al., 2004), and a synergistically reduced silencing of subtelomeric genes was observed when *src1*Δ was combined with the *yku70*Δ allele.

In addition to telomeres, Src1 is also associated with the rDNA locus. Both consist of repetitive sequences, which have to be protected from uncontrolled homologous recombination to maintain genomic integrity. Notably, Src1 was copurified with Lrs4, a factor located at the rDNA locus with a role in rDNA silencing and suppression of rDNA recombination (Huang et al., 2006). Lrs4 together with cohesin are thought to prevent the formation of chromatid junctions, and Src1 could aid in this step locally at the inner nuclear membrane. In line with a function together with cohesin, Src1 has been reported to be involved in sister chromatid separation and is genetically linked to S*CC1* and *ESP1* (Rodríguez-Navarro et al., 2002).

Our study further reveals that Src1 is required for proper gene expression of subtelomeric genes, such as several *PHO* genes, that are associated with the inner nuclear membrane. Transcription of *PHO* genes in response to the phosphate concentration is regulated by the phosphorylation status of the transcription factor Pho4, which in turn affects its nucleocytoplasmic shuttling (O'Neill et al., 1996). Our data suggest that the subtelomeric *PHO* genes may exhibit, besides specific control by Pho4, a global regulation as a result of their association with the inner nuclear membrane, which is repressive for gene expression. By which mechanism Src1 could affect subtelomeric gene expression remains unclear. It is known that in contrast to telomere silencing mediated by the Sir complex, silencing of genes within subtelomeric/HAST (Hda1-affected subtelomeric) domains depends on the local nucleosome structure (Wyrick et al., 1999). This is characterized by histone H3 hypomethylation and hypoacetylation (Bernstein et al., 2002; Robyr et al., 2002). Whether Src1 specifically affects histone modifications in subtelomeric regions remains to be determined, but its role in gene expression could be envisaged in a broader sense (e.g., by interfering with different types of mechanisms that activate or repress gene expression). The effect of both up- and down-regulation of genes observed in the *src1Δ* mutant could be caused by transcription factors concentrated at the nuclear periphery that act as both activators and repressors. Lack of Src1 might restrict the access of these factors to subtelomeric loci as a result of an altered chromatin structure. The macroarray data also show that expression of some genes that are not located at subtelomeric regions, but randomly across the chromosomes, were affected

by loss of *SRC1*. Because Src1 did not interact significantly with these genes according to ChIP-on-chip, the effect could be indirect (e.g., caused by misregulation of subtelomeric genes, which in turn alter expression of genes located elsewhere in the genome).

The finding that Src1 is genetically linked to factors of the THO–TREX and TREX-2 complexes suggested an involvement in transcription and/or export. However, the disruption of *SRC1* did not cause an mRNA export defect. Thus, Src1 could be connected to the transcription-assisted (upstream) functions of these TREX complexes. It is well established that mutations in these TREX factors (e.g., in Thp1, Sac3, and Hpr1) not only inhibit transcription elongation but also induce transcription-dependent hyperrecombination and genome instability (for review see Reed and Cheng, 2005). Src1 is not genetically linked to all of the subunits of THO–TREX and TREX-2, which suggests that the subunits within the TREX complexes may have different roles with respect to Src1 function. For example, Sub2, a subunit of THO–TREX, not only functions in transcription, splicing, and mRNA export but was also shown to be localized to telomeres and to affect heterochromatic gene expression (Lahue et al., 2005).

Collectively, the simplest model of how Src1 functions as an integral inner nuclear membrane protein is to help in recruiting and organizing the peripheral (telomeric and subtelomeric) chromatin, perhaps by directly binding to specific DNA sequences or nucleosomes (see above). By organizing subtelomeric and telomeric DNA in a distinct nuclear compartment, the nuclear periphery, Src1 could help to cluster a group of genes in a zone in which silencing factors, transcription activators, and repressors cooperate for regulated gene expression and which also has access to an efficient mRNA export pathway via the TREX machineries associated with NPCs. Subtelomeric and telomeric chromatin and the rDNA locus are repetitive, and their preservation is crucial for maintaining genome integrity. Thus, localization of this chromatin to the nuclear membrane could also play a role in preventing unwanted recombination. Many of these described functions attributed to Src1 can now be tested by exploiting *src1* mutants in different functional assays.

Last but not least, Src1 is related to higher eukaryotic LEM domain–containing inner nuclear membrane proteins that were shown to interact with transcription regulators (e.g., R-Smads and HDAC3) and thus affect gene expression and signal transduction by recruitment of transcription regulators to the nuclear periphery (for reviews see Gruenbaum et al., 2005; Wagner and Krohne, 2007). Our study showed that the LEM domain protein Src1 is associated with subtelomeric chromatin and affects gene expression in this region. Thus, Src1 could serve as a model protein to gain further insight into the complex role of inner nuclear membrane proteins, including their involvement in diseases such as laminopathies.

## Materials and methods

### Yeast strains and plasmid constructs

*S. cerevisiae* strains and plasmids are listed in Table S2 (available at http://www.jcb.org/cgi/content/full/jcb.200803098/DC1). The synthetic lethal screens were performed as described previously (Segref et al., 1997). In the *thp1*Δ screen, 54 synthetic lethal mutants were obtained from ~70,000 colonies. 24 of these mutants were complemented by plasmid-borne *THP1* and used for further analysis.

### Fluorescence microscopy

Cells were grown in selective medium at 30°C to logarithmic phase. Fluorescence microscopy was performed using an Imager Z1 (Carl Zeiss, Inc.) equipped with a 63× NA 1.4 Plan-Apochromat oil immersion lens (Carl Zeiss, Inc.) and using DICIII and HEeGFP filters. Pictures were acquired with a camera (AxioCamMRm; Carl Zeiss, Inc.) and AxioVision 4.3 software (Carl Zeiss, Inc.). Pictures were exported as jpg files and processed in PhotoShop 7.0 (Adobe) for levels.

### Src1 membrane extraction, topology analysis, and affinity purification

500 mg of spheroplasts prepared from early log-phase cultures were lysed with a Dounce homogenizer in 3 ml of buffer (150 mM NaCl and 20 mM Tris-HCl, pH 8.0) containing protease inhibitors and was pelleted at 2,000 rpm for 2 min. The supernatant was centrifuged at 13,000 rpm for 20 min at 4°C, resulting in pellet and supernatant. One fourth of the pellet was resuspended in 400 µl of buffer (1% Triton X-100 and 1 M NaCl or in 0.1 M sodium carbonate, pH 11.5), incubated 30 min on ice, and separated into a soluble and pellet fraction by ultracentrifugation at 100,000 *g* for 1 h at 4°C. Equal amounts were analyzed by Western blotting using anti-ProtA, anti-Vam3, and anti-Nsp1 antibodies.

The galactose promoter–driven TEV protease fused to NLS and a myc tag was integrated into strains expressing N- or C-terminal–tagged Src1 forms. An equivalent of 3 $OD_{600}$ of exponentially growing cells in YPD or YPG at 30°C was harvested, TCA lysis was performed, and equal amounts were analyzed by Western blotting using anti-ProtA, anti-myc, and anti-Arc1 antibodies. Affinity purification of ProtA-tagged bait Src1 was performed as described previously (Gavin et al., 2002).

### DNA macroarray measurement of RNA levels

50 ml of wt and *src1*Δ cells ($OD_{600}$ 0.5) were pelleted and immediately frozen. After thawing the samples on ice, total RNA was isolated and reverse transcribed using $^{33}$P-labeled deoxycytidine triphosphate and oligo d(5′-$T_{15}$VN-3′) (García-Martínez et al., 2004). Hybridization was performed on nylon filters using PCR-amplified whole ORF sequences as probes (Alberola et al., 2004; García-Martínez et al., 2004) except that hybridizations were 40–48 h. Three different cultures were used for each strain. Scanning and analysis of the macroarrays were performed essentially as described previously using ArrayStat software (García-Martínez et al., 2004; Rodríguez-Navarro et al., 2004). Apart from the genes detected by ArrayStat as significantly up- or down-regulated, we obtained an additional list of 16 genes that were expressed over background in the three replicates in *src1*Δ and below background in all three replicates in wt cells. Array data have been submitted to the Gene Expression Omnibus data repository (accession no. GSE6370).

### RNA isolation and real-time PCR

Cells were grown in selective HP medium (11 mM $KH_2PO_4$) at 30°C to an $OD_{600}$ of 0.5. Half of the cells was washed and grown for 2 h in selective LP medium (220 µM $KH_2PO_4$) at 30°C. Total RNA was isolated using the RNeasy Mini kit (QIAGEN). cDNA was synthesized from 1 µg of total RNA using the QuantiTect Reverse Transcription kit (QIAGEN). *PHO11*, *PHO12*, and *PHO84* cDNAs were detected by quantitative real-time PCR (ABI-Prism 7000; Applied Biosystems) using specific primers and TaqMan probes (Table S3, available at http://www.jcb.org/cgi/content/full/jcb.200803098/DC1). Triplicate reactions containing cDNA equivalent to 0.08 µg RNA were analyzed per experiment.

### ChIP-on-chip analysis

ChIP-on-chip analyses were performed as described previously (Cam et al., 2005) with minor modifications. Cells were grown in selective HP medium at 30°C to an $OD_{600}$ of 0.5. After washing, the cells were grown for 2 h in selective LP medium at 30°C. The PFA–dimethyl adipimidate cross-linked chromatin was sheared by sonication and without preclearing was incubated with IgG Sepharose 6 Fast Flow (GE Healthcare) for 2–3 h at 4°C. After extensive washing and amplification, we combined 500 ng Cy5-labeled ChIP DNA with an equal amount of Cy3-labeled whole cell extract DNA and hybridized it onto a 4 × 44 K *S. cerevisiae* Whole Genome ChIP-on-chip Microarray (Agilent Technologies). Hybridization, washes, and processing slides were performed in accordance with the yeast ChIP-on-chip protocol (version 9.1; Agilent Technologies).

For statistical analysis, we have taken a 10-kb region from the end of the chromosomes. The 599 independent probes representing subtelomeric regions show an average of 4.45× Src1 enrichment over the baseline. The remaining 40,881 probes give a 1.06× average enrichment. In the negative control (cells expressing only ProtA), we did not detect any enrichment of immunoprecipitated ProtA at telomeres, centromeres, HML

and HMR loci, or on rDNA (1.08× average enrichment at subtelomeric region vs. 1.03×).

### Localization of single chromosomal loci

Growing and mounting yeast cells for in vivo microscopy were performed as described previously (Cabal et al., 2006) using a Revolution Nipkow disk confocal system (Andor Technology). The system was controlled using Revolution IQ software (version 1.5; Andor Technology). Z stacks of 41 images with a 250-m Z step were acquired using a 100×/1.4 NA Plan Apochromat oil immersion objective (Carl Zeiss, Inc.). Pixel size was 77.3 nm. Quantitative analysis of microscopy data was performed using Matlab software as described previously (Cabal et al., 2006). In brief, each nucleus was processed to extract 3D coordinates of the locus, the nuclear center, and the nuclear envelope. In the following step, loci positions relative to the nuclear center obtained from different nuclei were plotted on the same 3D graph. Finally, and for reading facility, this 3D graph was projected on a 2D graph using radial projection (i.e., the loci–nuclear center distance is conserved; Cabal et al., 2006).

### Online supplemental material

Fig. S1 contains the localization of Src1 splice forms in wt and *nup133*Δ cells. Fig. S2 shows that Src1-L and Src1-S do not purify stoichiometric binding partners. Fig. S3 shows the genomic-wide distribution maps of Src1-L. Table S1 contains the up- and down-regulated genes in *src1*Δ cells. Table S2 indicates the yeast strains and plasmids used, and Table S3 presents the real-time PCR primers used in this study. Online supplemental material is available at http://www.jcb.org/cgi/content/full/jcb.200803098/DC1.

We thank Dr. Christian Ungermann for providing the anti-Vam3 antibody and Dr. Frank Uhlmann for providing the $P_{GAL}$::NLS-myc9-TEV-2xNLS construct. We thank Dr. Katja Strässer for performing the *hpr1*Δ screen and Sheila Lutz, Dr. Dieter Kressler, and Jonas Binding for discussions. We thank Axel B. Berger, Dr. Christophe Zimmer, and Dr. Olivier Gadal for sharing unpublished data, providing yeast strains, and providing access to bioinformatics tools. We wish to thank Vicent Pelechano for his advice with the macroarray data analysis.

The work in J.E. Perez-Ortin's laboratory was funded by Ministerio de Educación y Ciencia (Spain) with grants BFU2006-15446-C03-02/BMC and BFU2007-67575-C03-01/BMC. G.G. Cabal was a recipient of the fellowship of Association pour la Recherche sur le Cancer. E. Hurt was a recipient of grants from the Deutsche Forschungsgemeinschaft (SFB638 and B3).

Submitted: 18 March 2008
Accepted: 8 August 2008

## References

Akhtar, A., and S.M. Gasser. 2007. The nuclear envelope and transcriptional control. *Nat. Rev. Genet.* 8:507–517.

Alberola, T.M., J. García-Martínez, O. Antúnez, L. Viladevall, A. Barcelo, J. Ariño, and J.E. Pérez-Ortín. 2004. A new set of DNA macrochips for the yeast *Saccharomyces cerevisiae*: features and uses. *Int. Microbiol.* 7:199–206.

Askree, S.H., T. Yehuda, S. Smolikov, R. Gurevich, J. Hawk, C. Coker, A. Krauskopf, M. Kupiec, and M.J. McEachern. 2004. A genome-wide screen for *Saccharomyces cerevisiae* deletion mutants that affect telomere length. *Proc. Natl. Acad. Sci. USA.* 101:8658–8663.

Bernstein, B.E., E.L. Humphrey, R.L. Erlich, R. Schneider, P. Bouman, J.S. Liu, T. Kouzarides, and S.L. Schreiber. 2002. Methylation of histone H3 Lys 4 in coding regions of active genes. *Proc. Natl. Acad. Sci. USA.* 99:8695–8700.

Brachner, A., S. Reipert, R. Foisner, and J. Gotzmann. 2005. LEM2 is a novel MAN1-related inner nuclear membrane protein associated with A-type lamins. *J. Cell Sci.* 118:5797–5810.

Bupp, J.M., A.E. Martin, E.S. Stensrud, and S.L. Jaspersen. 2007. Telomere anchoring at the nuclear periphery requires the budding yeast Sad1-UNC-84 domain protein Mps3. *J. Cell Biol.* 179:845–854.

Cabal, G.G., A. Genovesio, S. Rodríguez-Navarro, C. Zimmer, O. Gadal, A. Lesne, H. Buc, F. Feuerbach-Fournier, J.C. Olivo-Marin, E.C. Hurt, and U. Nehrbass. 2006. SAGA interacting factors confine sub-diffusion of transcribed genes to the nuclear envelope. *Nature.* 441:770–773.

Cai, M., Y. Huang, R. Ghirlando, K.L. Wilson, R. Craigie, and G.M. Clore. 2001. Solution structure of the constant region of nuclear envelope protein LAP2 reveals two LEM-domain structures: one binds BAF and the other binds DNA. *EMBO J.* 20:4399–4407.

Cam, H.P., T. Sugiyama, E.S. Chen, X. Chen, P.C. FitzGerald, and S.I. Grewal. 2005. Comprehensive analysis of heterochromatin- and RNAi-mediated epigenetic control of the fission yeast genome. *Nat. Genet.* 37:809–819.

Caputo, S., J. Couprie, I. Duband-Goulet, E. Kondé, F. Lin, S. Braud, M. Gondry, B. Gilquin, H.J. Worman, and S. Zinn-Justin. 2006. The carboxyl-terminal nucleoplasmic region of MAN1 exhibits a DNA binding winged helix domain. *J. Biol. Chem.* 281:18208–18215.

Davis, C.A., L. Grate, M. Spingola, and M. Ares Jr. 2000. Test of intron predictions reveals novel splice sites, alternatively spliced mRNAs and new introns in meiotically regulated genes of yeast. *Nucleic Acids Res.* 28:1700–1706.

Fischer, T., K. Strässer, A. Rácz, S. Rodríguez-Navarro, M. Oppizzi, P. Ihrig, J. Lechner, and E. Hurt. 2002. The mRNA export machinery requires the novel Sac3p-Thp1p complex to dock at the nucleoplasmic entrance of the nuclear pores. *EMBO J.* 21:5843–5852.

Fischer, T., S. Rodríguez-Navarro, G. Pereira, A. Rácz, E. Schiebel, and E. Hurt. 2004. Yeast centrin Cdc31 is linked to the nuclear mRNA export machinery. *Nat. Cell Biol.* 6:840–848.

Gallardo, M., and A. Aguilera. 2001. A new hyperrecombination mutation identifies a novel yeast gene, THP1, connecting transcription elongation with mitotic recombination. *Genetics.* 157:79–89.

García-Martínez, J., A. Aranda, and J.E. Pérez-Ortín. 2004. Genomic run-on evaluates transcription rates for all yeast genes and identifies gene regulatory mechanisms. *Mol. Cell.* 15:303–313.

Gavin, A.C., M. Bösche, R. Krause, P. Grandi, M. Marzioch, A. Bauer, J. Schultz, J.M. Rick, A.M. Michon, C.M. Cruciat, et al. 2002. Functional organization of the yeast proteome by systematic analysis of protein complexes. *Nature.* 415:141–147.

Gruenbaum, Y., A. Margalit, R.D. Goldman, D.K. Shumaker, and K.L. Wilson. 2005. The nuclear lamina comes of age. *Nat. Rev. Mol. Cell Biol.* 6:21–31.

Hediger, F., F.R. Neumann, G. Van Houwe, K. Dubrana, and S.M. Gasser. 2002. Live imaging of telomeres: yKu and Sir proteins define redundant telomere-anchoring pathways in yeast. *Curr. Biol.* 12:2076–2089.

Huang, J., I.L. Brito, J. Villen, S.P. Gygi, A. Amon, and D. Moazed. 2006. Inhibition of homologous recombination by a cohesin-associated clamp complex recruited to the rDNA recombination enhancer. *Genes Dev.* 20:2887–2901.

King, M.C., C.P. Lusk, and G. Blobel. 2006. Karyopherin-mediated import of integral inner nuclear membrane proteins. *Nature.* 442:1003–1007.

Klein, F., T. Laroche, M.E. Cardenas, J.F. Hofmann, D. Schweizer, and S.M. Gasser. 1992. Localization of RAP1 and topoisomerase II in nuclei and meiotic chromosomes of yeast. *J. Cell Biol.* 117:935–948.

Köhler, A., and E. Hurt. 2007. Exporting RNA from the nucleus to the cytoplasm. *Nat. Rev. Mol. Cell Biol.* 8:761–773.

Köhler, A., P. Pascual-García, A. Llopis, M. Zapater, F. Posas, E. Hurt, and S. Rodríguez-Navarro. 2006. The mRNA export factor Sus1 is involved in Spt/Ada/Gcn5 acetyltransferase-mediated H2B deubiquitinylation through its interaction with Ubp8 and Sgf11. *Mol. Biol. Cell.* 17:4228–4236.

Kyte, J., and R.F. Doolittle. 1982. A simple method for displaying the hydropathic character of a protein. *J. Mol. Biol.* 157:105–132.

Lahue, E., J. Heckathorn, Z. Meyer, J. Smith, and C. Wolfe. 2005. The *Saccharomyces cerevisiae* Sub2 protein suppresses heterochromatic silencing at telomeres and subtelomeric genes. *Yeast.* 22:537–551.

Laroche, T., S.G. Martin, M. Gotta, H.C. Gorham, F.E. Pryde, E.J. Louis, and S.M. Gasser. 1998. Mutation of yeast Ku genes disrupts the subnuclear organization of telomeres. *Curr. Biol.* 8:653–656.

Lei, E.P., C.A. Stern, B. Fahrenkrog, H. Krebber, T.I. Moy, U. Aebi, and P.A. Silver. 2003. Sac3 is an mRNA export factor that localizes to cytoplasmic fibrils of nuclear pore complex. *Mol. Biol. Cell.* 14:836–847.

Louis, E.J. 1995. The chromosome ends of *Saccharomyces cerevisiae*. *Yeast.* 11:1553–1573.

Mans, B.J., V. Anantharaman, L. Aravind, and E.V. Koonin. 2004. Comparative genomics, evolution and origins of the nuclear envelope and nuclear pore complex. *Cell Cycle.* 3:1612–1637.

O'Neill, E.M., A. Kaffman, E.R. Jolly, and E.K. O'Shea. 1996. Regulation of PHO4 nuclear localization by the PHO80-PHO85 cyclin-CDK complex. *Science.* 271:209–212.

Oshima, Y. 1997. The phosphatase system in *Saccharomyces cerevisiae*. *Genes Genet. Syst.* 72:323–334.

Reed, R., and H. Cheng. 2005. TREX, SR proteins and export of mRNA. *Curr. Opin. Cell Biol.* 17:269–273.

Robyr, D., Y. Suka, I. Xenarios, S.K. Kurdistani, A. Wang, N. Suka, and M. Grunstein. 2002. Microarray deacetylation maps determine genome-wide functions for yeast histone deacetylases. *Cell.* 109:437–446.

Rodríguez-Navarro, S., J.C. Igual, and J.E. Pérez-Ortín. 2002. SRC1: an intron-containing yeast gene involved in sister chromatid segregation. *Yeast.* 19:43–54.

Rodríguez-Navarro, S., T. Fischer, M.J. Luo, O. Antúnez, S. Brettschneider, J. Lechner, J.E. Pérez-Ortín, R. Reed, and E. Hurt. 2004. Sus1, a functional component of the SAGA histone acetylase complex and the nuclear pore-associated mRNA export machinery. *Cell.* 116:75–86.

Segref, A., K. Sharma, V. Doye, A. Hellwig, J. Huber, R. Luhrmann, and E. Hurt. 1997. Mex67p, a novel factor for nuclear mRNA export, binds to both poly(A)+ RNA and nuclear pores. *EMBO J.* 16:3256–3271.

Sommer, P., and U. Nehrbass. 2005. Quality control of messenger ribonucleoprotein particles in the nucleus and at the pore. *Curr. Opin. Cell Biol.* 17:294–301.

Taddei, A., F. Hediger, F.R. Neumann, C. Bauer, and S.M. Gasser. 2004. Separation of silencing from perinuclear anchoring functions in yeast Ku80, Sir4 and Esc1 proteins. *EMBO J.* 23:1301–1312.

Wagner, N., and G. Krohne. 2007. LEM-domain proteins: new insights into lamin-interacting proteins. *Int. Rev. Cytol.* 261:1–46.

Wu, W., F. Lin, and H.J. Worman. 2002. Intracellular trafficking of MAN1, an integral protein of the nuclear envelope inner membrane. *J. Cell Sci.* 115:1361–1371.

Wyrick, J.J., F.C. Holstege, E.G. Jennings, H.C. Causton, D. Shore, M. Grunstein, E.S. Lander, and R.A. Young. 1999. Chromosomal landscape of nucleosome-dependent gene expression and silencing in yeast. *Nature.* 402:418–421.